Principal modes of variability of Martian atmospheric surface pressure

S. S. Leroy,[1] Y. L. Yung,[2] M. I. Richardson,[2] and R. J. Wilson[3]

[1]   An analysis of daily-to-interannual variability in the surface pressure field of the Martian nothern hemisphere as given by a Martian climate model is presented. In an empirical orthogonal function (EOF) decomposition, the dominant first two modes of variability comprise a zonal wavenumber 1 feature centered at 70 N latitude moving eastward with a period of 6 to 8 sols. This feature is a baroclinic wave and accounts for 53% of the northern hemisphere non-stationary surface pressure variability, and, when active, has an amplitude of up to 2% of local surface pressure. The third mode of the EOF decomposition is annular about the Martian north pole, is null southward of 70 N, and accounts for 7% of the northern hemisphere non-stationary surface pressure variability. The baroclinic wave (EOFs 1 & 2) is active during northern hemisphere winter and spring, consistent with models of the Martian atmospheric circulation, and the annular mode (EOF 3) is active only at the onset and demise of the baroclinic feature. When active, it is not uncommon for the annular mode to reside in either its positive or negative state stably for 20 to 30 sols. It is postulated that baroclinic waves with longitudinal wavenumber 2, 3, and 4 act as a pump for the annular mode. The annular mode should not be present in MGS TES data.   INDEX TERMS: 1610 Global Change: Atmosphere (0315, 0325); 1620 Global Change: Climate dynamics (3309); 3346 Meteorology and Atmospheric Dynamics: Planetary meteorology (5445, 5739); 5409 Planetology: Solid Surface Planets: Atmospheres—structure and dynamics. **Citation:** Leroy, S. S., Y. L. Yung, M. I. Richardson, and R. J. Wilson, Principal modes of variability of Martian atmospheric surface pressure, *Geophys. Res. Lett.*, *30*(13), 1707, doi:10.1029/2002GL015909, 2003.

1.   Introduction

[2]   The Arctic Oscillation (AO) in the Earth's atmosphere was discovered by an empirical orthogonal function (EOF) decomposition of the atmosphere's surface pressure field and the upper air height fields of the NCEP Reanalysis [*Kalnay et al.*, 1996; *Thompson and Wallace*, 2000; *Thompson et al.*, 2000]. It is, in fact, the dominant mode of daily-interannual variability in the Earth's northern hemisphere surface pressure field, accounting for ca. 22% of the total variance. The AO is thought to be the global manifestation of the North Atlantic Oscillation (NAO), a key player in determining the intensity of the western European winter [*Thompson and Wallace*, 2001].

It is of interest to find similar phenomena in the atmospheres of other planets.

[3]   In the case of Mars, the intra-annual surface pressure variability is dominated by the seasonal cycle followed by wintertime baroclinic waves in the northern hemisphere. The mass of the Martian atmosphere is volatile, so the annual cycle of Martian surface pressure is much larger than the terrestrial surface pressure [*Hess et al.*, 1980]. During northern winter, baroclinic waves dominate daily surface pressure variability. The waves' existence has been predicted [*Leovy and Mintz*, 1969], their characteristics described by linear instability theory [*Barnes*, 1984] and atmospheric modeling [*Barnes et al.*, 1993], and observed in the upper air [*Banfield et al.*, 2003]. The presence of these waves suggests the possibility of a north-polar annular mode much like the Earth's Arctic Oscillation, especially if planetary waves play a significant role in the AO's mechanism [*Hartmann et al.*, 2000]. We investigate whether such an annular mode exists in Mars' atmosphere and, if so, what waves might be responsible.

[4]   In this paper we perform an EOF decomposition as *Thompson and Wallace* [2000] did in discovering the AO but for the Martian atmosphere. Since no atmospheric analysis exists for the Martian atmosphere, we analyze the output of a Martian general circulation model (GCM). This analysis should serve as a tool for comparative planetology and help in the understanding of mechanisms of climate variability throughout the solar system.

2.   Analysis

[5]   We used the surface pressure output of the Mars GCM developed from the GFDL SKYHI model [*Wilson and Hamilton*, 1996]. This model has 5°-by-6° latitude-longitude resolution and 20 hybrid vertical levels. The control run used here generated two-sol averages for approximately six and a half Martian years (2160 time increments, 668 sols per Martian year). The dust distribution is variable with the optical depth approximately 0.5 as in *Wilson and Hamilton* [1996]. The results are no different when using a control run with dust optical depth fixed at 0.5.

[6]   The surface pressure (p_s) on Mars is dominated by the annual cycle which causes p_s to vary from 6 to 10 hPa. Also, the topography of Mars is more exaggerated than on Earth, the departures from a mean areoid being a few kilometers on hemispheric scales [*Smith et al.*, 2001]. For these reasons, we work with the logarithm of the surface pressure and remove the annual cycle from the ln p_s timeseries after first computing it as a function of sol-of-year. Deviations in ln p_s can then be interpreted as fractional changes in the surface pressure. Since the model output is bidaily and the annual cycle is subtracted by sol-
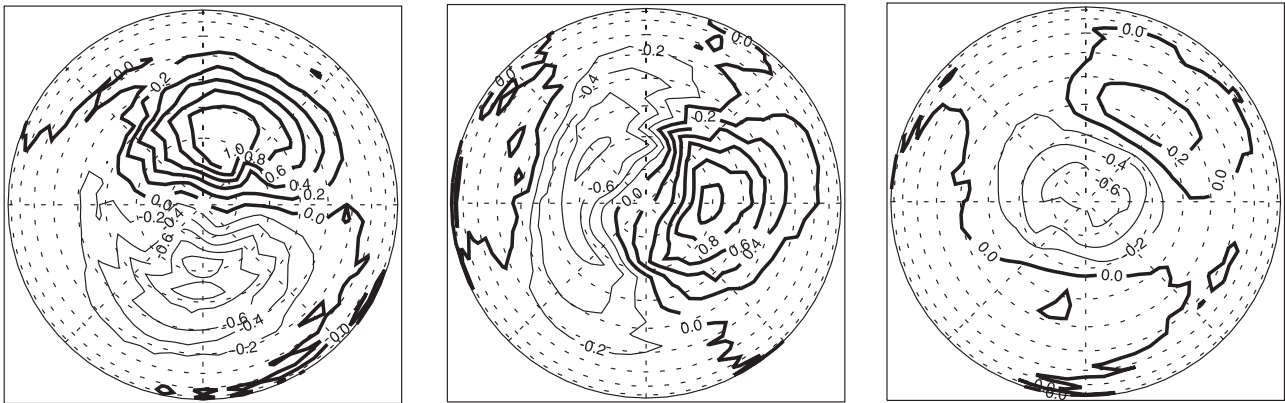
[1]Jet Propulsion Laboratory, California Institute of Technology, Pasadena, California, USA.
[2]Division of Geological and Planetary Sciences, California Institute of Technology, Pasadena, California, USA.
[3]Geophysical Fluid Dynamics Laboratory, Princeton, New Jersey, USA.

Figure 1. The first three empirical orthogonal functions of the logarithm of the surface pressure of Mars, mean annual cycle removed. The output is from the GFDL general circulation model of the Martian atmosphere. The units are per cent of surface pressure with the contours separated by 0.2%. Thick contours are of positive values. Martian surface pressure ranges from 6 hPa to 10 hPa depending on season.

of-year, neither the atmospheric tides nor the stationary waves so prominent in Mars' atmosphere are manifested in this analysis.

[7] The computation of EOFs is done using standard eigenvalue/eigenvector techniques. The domain of analysis is the entire northern hemisphere, the full timeseries is used, and the area weighting is done by the solid angle of Martian surface represented by each model gridpoint. As a consequence, the units of each EOF $\mathbf{e}_\mu$ are steradian$^{-1/2}$ and the units of its associated eigenvalue λ_μ are $[\delta \ln p_s]^2$ steradian. Multiply by 10^4 to get (per cent)^2 steradian. The principal component timeseries have the units of $\lambda_\mu^{1/2}$.

[8] The total daily-to-interannual northern hemisphere $\delta \ln p_s$ variance is 1.867 (per cent)^2 steradian. The eigenvalues (λ_μ) of the first three EOFs are 0.633, 0.476, and 0.127 (per cent)^2 steradian. In Figure 1 we present the first three scaled EOFs ($\lambda_\mu^{1/2}\mathbf{e}_\mu$) of northern hemisphere surface pressure variability. The first scaled EOF has extrema of ±1.2% between 65 and 70 N latitude and is wavenumber 1 in longitudinal structure. Likewise, the second EOF has extrema of ±1.0% in the same latitude band and is also wavenumber 1 in longitudinal structure. Taken together, they represent 53% of the northern hemisphere (non-stationary) $\delta \ln p_s$ variability. By contrast, the (non-stationary) variance in $\delta \ln p_s$ in the southern hemisphere is 0.529 (per cent)^2 steradian, and the southern hemisphere EOFs contain none of the well-defined features of the northern hemisphere EOFs, a known asymmetry [*Barnes et al.*, 1993].

[9] The third scaled EOF of Figure 1 is annular about the north pole, with a minimum of −0.6% at the pole. In the seasons it is most active it reaches an amplitude of 1.8% at the pole. It decays to zero at 60 N and remains only slightly positive south of 60 N. This mode is reminiscent of the Arctic Oscillation (AO) in the Earth's atmosphere. Its positive (negative) phase represents a strengthening (weakening) of the north polar vortex. Thus, an 8-hPa atmosphere will contain EOF 3 fluctuations of 14 Pa between the pole and 60 N latitude. The depth of the wintertime polar vortex reaches 240 Pa (from 70 N to the pole) on average, so fluctuations of EOF 3 amount to a 6% variation in the intensity of the north polar vortex. While there is no preferred frequency of EOF 3, once or twice during its

active seasons it can persist in either its high or low states for periods of 20 to 30 sols (see Figure 2b), suggesting that EOF 3 may be associated with stable states.

[10] We analyzed the principal component timeseries of the first three EOFs, PC$_1(t)$, PC$_2(t)$, and PC$_3(t)$. See (Figures 2a and 2b) for L_s 90° of the second year to 90° of the third year. In the inset of (a) we show that in northern winter PC$_2$ leads PC$_1$ by 90°, indicating eastward propagation of a longitudinal wavenumber 1 wave, EOFs 1 and 2 being quadrature components of the same wave. In order to
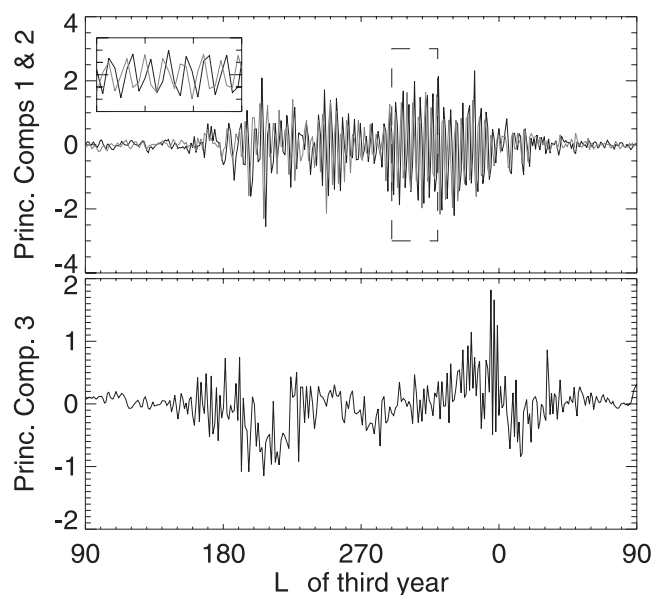

Figure 2. Northern hemisphere activity plots. In (a) is shown the principal component timeseries for EOFs 1 & 2 with units of (per cent) steradian$^{1/2}$. PC 1 is the dark curve, and PC 2 is the lighter curve. The inset is an expansion between L_S 290 and 320. In (b) is shown the principal component timeseries for EOF 3, the annular mode. The units are roughly equivalent to surface pressure fluctuation in per cent at 70 N for (a), at the north pole for (b). The abscissa is solar longitude in the third year of the run.

estimate the propagation characteristics of this wave, we Fourier analyzed the complex timeseries $PC_1(t) + i\ PC_2(t)$ and found a pronounced eastward propagating wave with a periodicity of 6 to 8 sols. Modeling has shown this feature to represent a baroclinic wave in early northern winter and a Rossby wave in late northern winter [*Wilson et al.*, 2002]. It is also consistent with Viking lander data [*Barnes*, 1980, 1981; *Collins et al.*, 1996].

[11] The variability associated with EOF 3 occurs only at the onset and demise of the wave activity associated with EOFs 1 and 2 (L_s 180° and 0°), as is illustrated in Figure 3. This corresponds to late northern fall and early northern spring. The baroclinic wavenumber 1 feature of EOFs 1 and 2 is active throughout the northern fall, winter and spring. If wave activity is a condition for activity of the annular EOF 3 as is implied by *Hartmann et al.* [2000] for the Earth's AO, then the wavenumber 1 feature of EOFs 1 and 2 cannot be the sole cause since the wave is present throughout northern fall through spring.

[12] While the temporal resolution of the model output is too coarse to resolve the frequency/phase speed of higher order baroclinic disturbances in the northern midlatitudes, it nevertheless remains possible to calculate their seasonal amplitudes. We do this by removing the annual cycle, Fourier analyzing the $\ln p_s$ anomaly at 70 N latitude for each time increment, squaring the results to obtain power, and averaging over the 6.5 Martian years of the run. On average, the wavenumber 1 fluctuations account for 81% of the variance at 70 N latitude, wavenumber 2 for 12%, wavenumber 3 for 4%, and wavenumber 4 for 1%. The variability of the wavenumber 2 and 3 waves is significantly underrepresented because their periodicity is approximately harmonic with the two-sol sampling of this study [*Wilson*, 2000]. In Figure 3 it is apparent that the seasonal activity of the wavenumber 2, 3, and 4 anomalies coincides with the activity of EOF 3 better than with the activity of the baroclinic feature of EOFs 1 and 2.

[13] In order to determine whether there is a signature of the third EOF in data from the MGS TES experiment, we simulate the sum of the two TES channels on either side of the center of the CO_2 15 μm feature. This simulation is representative of mid-tropospheric temperature. We regress the TES T_B timeseries on the PC_1, PC_2, and PC_3 timeseries (see Figure 2). The regression maps are shown in Figure 4. Given that the wavenumber 1 baroclinic feature of EOFs 1 and 2 propagates eastward, the temperature anomaly associated with the baroclinic wave leads the pressure fluctuation by 90°. On the other hand, there is no clear T_B anomaly associated with surface pressure EOF 3, indicating that the annular AO-like mode would not be apparent in MGS TES data. Because PC_3 does not regress onto T_B, empirically there is likely no upper air temperature anomaly associated with EOF 3 of $\ln p_s$.

3. Discussion

[14] The presence of an arctic oscillation in the Martian climate offers an interesting topic for comparative planetology. In the Earth's atmosphere there are fundamental differences in the character of planetary waves between the northern and southern hemispheres yet annular modes exist in both [*Thompson and Solomon*, 2002], thus raising
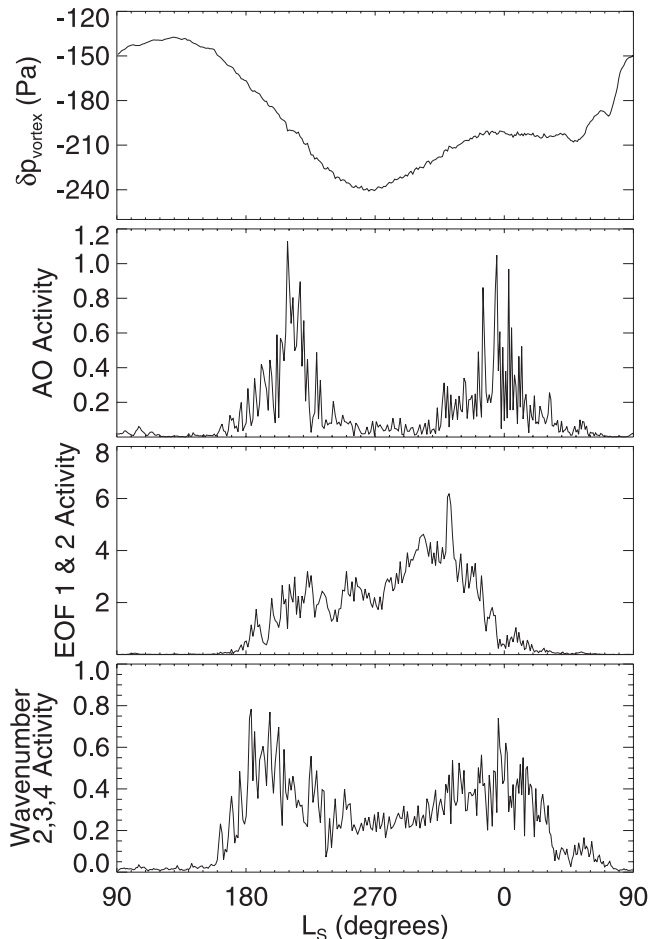

Figure 3. Annual cycle of northern vortex, EOF 3 activity, EOFs 1 and 2 activity, and wavenumber 2, 3, 4 activity. The top plot shows the depth of the northern polar vortex as surface pressure at 90 N latitude less the surface pressure at 70 N latitude. More negative numbers imply a stronger vortex and a more baroclinically unstable front at the boundary of the Hadley cell and the north polar vortex. The second plot shows the variance associated with EOF 3 in units of (per cent)² steradian. These units correspond approximately to per cent fluctuation in surface pressure at the north pole. The third plot shows the variance associated with the first two EOFs, in the same units as those of EOF 3 activity. Each unit of (per cent)² steradian approximately corresponds to a (per cent)² in surface pressure variance at 70 N latitude. The fourth plot is of the combined variance associated with wavenumber 2, 3, and 4 travelling anomalies at 70 N latitude in units of (per cent)² in surface pressure. The abscissa is solar longitude.

the question of whether there is just one mechanism responsible for an annular EOF in surface pressure. In the case of the Martian atmosphere, the baroclinicity in the northern winter is much stronger than in the Earth's atmosphere [*Haberle et al.*, 1993; *Barnes et al.*, 1993].

[15] Why the annular EOF is most active during the beginning and ending of northern winter-spring is not understood. In the case of the Earth's AO, each state of the AO is thought to be dependent on whether the planetary scale wave activity directs EP flux toward the equator or
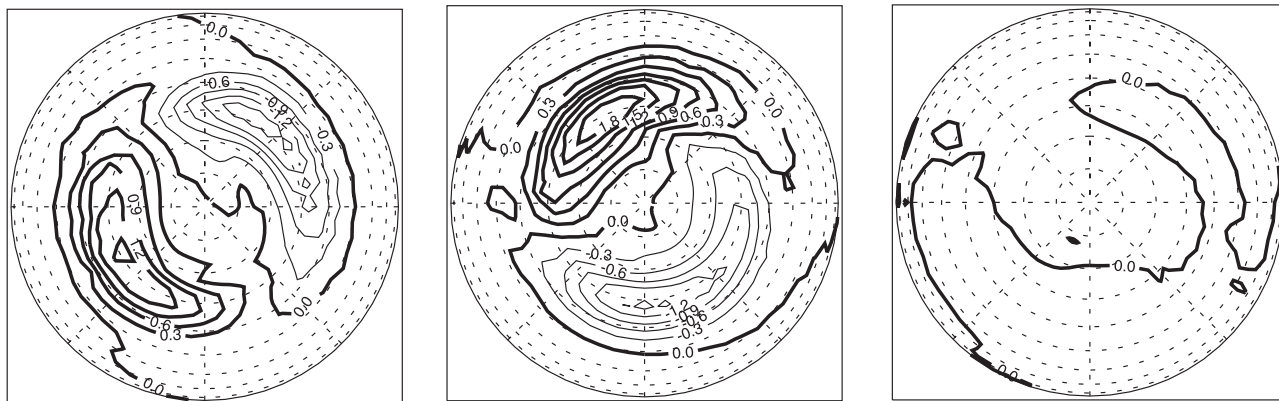
Figure 4. Regression of simulated MGS TES brightness temperature (T_B) on principal component timeseries 1, 2, and 3 of ln p_s variability. The units are K. Contours are in intervals of 0.3 K, and positive contours are thick.

toward the pole [*Lorenz and Hartmann*, 2001], which the wave activity does alternatively throughout northern winter. For Mars, because the activity of EOF 3 does not coincide with the wavenumber 1 wave as well as with wavenumber 2, 3, and 4 waves (at 70 N), it seems unlikely that it plays a role in driving EOF 3. On the other hand, the wavenumber 2, 3, and 4 waves are better candidates for a role in the mechanism of EOF 3 activity. An analysis of eddy fluxes and their interaction with the EOF 3, as produced by a higher temporal resolution run of a Mars GCM, is necessary to address issues raised here should the mechanism of a Martian AO be like that of the Earth's AO.

[16] After a regression analysis of simulated MGS TES brightness temperature representative of the mid-troposphere on the principal component timeseries of the log surface pressure EOFs, it is clear that the baroclinic wave of EOFs 1 and 2 should be apparent in MGS TES data and that the annular EOF 3 should not be apparent in MGS TES data. Further analysis is needed to explain this curious characteristic. Empirically, there may be little or no upper air anomaly associated with EOF 3 activity.

References

Banfield, D., B. Conrath, J. Pearl, M. Smith, P. Christensen, and R. Wilson, Forced waves in the Martian atmosphere from MGS TES nadir data, *Icarus*, 2003.

Barnes, J., Time spectral analysis of midlatitude disturbances in the Martian atmosphere, *J. Atmos. Sci.*, *37*, 2002–2015, 1980.

Barnes, J., Mid-latitude disturbances in the Martian atmosphere—a 2nd Mars year, *J. Atmos. Sci.*, *38*, 225–234, 1981.

Barnes, J., Linear baroclinic instability in the Martian atmosphere, *J. Geophys. Res.*, *41*, 1536–1550, 1984.

Barnes, J., J. Pollack, R. Haberle, C. Leovy, R. Zurek, H. Lee, and J. Schaeffer, Mars atmospheric dynamics as simulated by the NASA Ames general-circulation model. 2. Transient baroclinic eddies, *J. Geophys. Res.*, *98*, 3125–3148, 1993.

Collins, M., S. Lewis, P. Read, and F. Hourdin, Baroclinic wave transitions in the Martian atmosphere, *Icarus*, *120*, 344–357, 1996.

Haberle, R., J. Pollack, J. Barnes, R. Zurek, C. Leovy, J. Murphy, H. Lee, and J. Schaeffer, Mars atmospheric dynamics as simulated by the NASA Ames general-circulation model. 1. the zonal-mean circulation, *J. Geophys. Res.*, *98*, 3093–3123, 1993.

Hartmann, D., J. Wallace, V. Limpasuvan, D. Thompson, and J. Holton, Can ozone depletion and global warming interact to produce rapid climate change?, *Proc. Nat. Acad. Sci.*, *97*, 1412–1417, 2000.

Hess, S., J. Ryan, J. Tillman, R. Henry, and C. Leovy, The annual cycle of pressure on Mars measured by Viking-lander-1 and Viking-lander-2, *Geophys. Res. Lett.*, *7*, 197–200, 1980.

Kalnay, E., et al., The NCEP/NCAR 40-year reanalysis project, *Bull. Amer. Meteor. Soc.*, *77*, 437–471, 1996.

Leovy, C., and Y. Mintz, Numerical simulation of the atmospheric circulation and climate of Mars, *J. Atmos. Sci.*, *26*, 1167–1190, 1969.

Lorenz, D., and D. Hartmann, Eddy-zonal flow feedback in the southern hemisphere, *J. Atmos. Sci.*, *58*, 3312–3327, 2001.

Smith, D., et al., Mars Orbiter Laser Altimeter: Experiment summary after the first year of global mapping of Mars, *J. Geophys. Res.*, *106*, 23,689–23,722, 2001.

Thompson, D., and S. Solomon, Interpretation of recent southern hemisphere climate change, *Science*, *296*, 895–899, 2002.

Thompson, D., and J. Wallace, Annular modes in the extratropical circulation. Part I: Month-to-month variability, *J. Climate*, *13*, 1000–1016, 2000.

Thompson, D., and J. Wallace, Regional climate impacts of the northern hemisphere annular mode, *Science*, *293*, 85–89, 2001.

Thompson, D., J. Wallace, and G. Hegerl, Annular modes in the extratropical circulation. Part II: Trends, *J. Climate*, *13*, 1018–1036, 2000.

Wilson, R., Evidence for diurnal period Kelvin waves in the Martian atmosphere from Mars Global Surveyor TES data, *Geophys. Res. Lett.*, *27*, 3889–3892, 2000.

Wilson, R., and K. Hamilton, Comprehensive model simulation of thermal tides in the Martian atmosphere, *J. Atmos. Sci.*, *53*, 1290–1326, 1996.

Wilson, R. I., D. Banfield, B. J. Conrath, and M. D. Smith, Traveling waves in the Northern Hemisphere of Mars, *Geophys. Res. Lett.*, *29*(14), 1684, doi:10.1029/2002GL014866, 2002.

————————————

S. S. Leroy, Jet Propulsion Laboratory, California Institute of Technology, 4800 Oak Grove Dr., Pasadena, California 91109, USA. (Stephen.Leroy@jpl.nasa.gov)

Y. L. Yung and M. I. Richardson, Division of Geological and Planetary Sciences, California Institute of Technology, Pasadena, California, USA.

R. J. Wilson, Geophysical Fluid Dynamics Laboratory, Princeton, New Jersey, USA.